Journal of Electronic Imaging 14(1), 000 (Apr–Jun 2005)

New instantaneous frequency estimation method based on image processing techniques

Monica Borda
Technical University
Cluj-Napoca
Romania

Ioan Nafornita
Dorina Isar
Alexandru Isar
E-mail: isar@etc.utt.ro
"Politehnica" University, Timisoara, Romania

Abstract. *The aim of this paper is to present a new method for the estimation of the instantaneous frequency of a frequency modulated signal, corrupted by additive noise. Any time-frequency representation of an acquired signal is concentrated around the instantaneous frequency law of its useful component (the projection of the ridges of the time-frequency representation on the time-frequency plane) and realizes the diffusion of its noise component. So, extracting the ridges of the time-frequency representation, the instantaneous frequency of its useful component can be estimated. In this paper a new time-frequency representation is proposed. Using the image of this new time-frequency representation, its ridges can be extracted with the aid of some mathematical morphology operators. This is a ridges detection mechanism producing the projection on the time-frequency plane. This projection represents the result of the proposed estimation method. Some simulations prove the qualities of this method.* © *2005 SPIE and IS&T.* [DOI: 10.1117/1.1901677]

1 Introduction

The signals analyzed in this paper have low signal to noise ratios (SNR). The estimation of the instantaneous frequency (IF) of a monocomponent signal, not corrupted by noise, is a problem already solved.[1,2] When the useful part of the acquired signal is a multicomponent or it is perturbed by additive noise, the estimation problem is more complicated. Generally, methods based on the use of time-frequency representations (TFR) are used to solve this problem.[3,4] These distributions have two useful properties:

1. They have a very good concentration around the curve of the IF of the analyzed signal;[5]
2. They realize a diffusion of the perturbation noise power in the time-frequency plane (TFP).

So, computing the TFR of the analyzed signal: $x(t)=s(t)+n(t)$, where $n(t)$ is the perturbation, a good estimation of the ridges of the TFR of the signal $s(t)$ can be obtained. Projecting these ridges on the TFP, the IF of the signal $s(t)$ can be estimated. The quality of this estimator depends on the TFR and on the projection mechanism used. There are many methods to estimate the ridges of a TFR.[6] We propose here a new method, based on the use of mathematical morphology. The TFR obtained is regarded as an image and the estimation of its ridges is realized using image-processing techniques. This paper has the following structure: Sec. 2 analyzes the role of the TFRs in the implementation of the method of IF estimation. There are two TFR classes, linear and bilinear. Every class has some useful properties. To profit of the advantages of each class, a new TFR, based on the cooperation of linear and bilinear TFRs is proposed. The selection of the representatives TFRs, that cooperates in the new TFR, is accomplished to optimize the IF estimation. The role of the mathematical morphology operators is analyzed in Sec. 3. The aim of this paper, the algorithm of the new estimation method and its expected performances, are presented in Sec. 4. Section 5 is dedicated to simulation results. The conclusions are presented in Sec. 6.

Paper 03144 received Oct. 21, 2003; revised manuscript received May 6, 2004; accepted for publication Oct. 29, 2004.
1017-9909/2005/$22.00 © 2005 SPIE and IS&T.

2 The Role of the Time-Frequency Representations

The role of the TFRs in our estimation method is to spread the noise in the TFP and to locate the IF of the useful signal. There are a lot of TFRs, the short-time Fourier transform, the wavelet transform (linear representations), and the members of the Cohen class (bilinear representations). Every class of TFRs has its advantages. A new TFR, based on the cooperation between two TFRs, one linear and the other bilinear, is proposed in this paper. The selection of these two TFRs is realized to maximize the noise spreading effect. The definition of a linear TFR is the following:

If the conditions:

(1) $A \subset R^n$, $K: R \times A \rightarrow C$;

(2) $(\forall) a \in A$, $\tau \rightarrow K(\tau, a)$ is measurable and $\int_{-\infty}^{\infty} |K(\tau,a)|^2 d\tau = 1$;

(3) $(\forall)\omega\in R,\ a\to\Im\{K(\tau,a)\}(\omega)$ is measurable and $\int_A|\Im\{K(\tau,a)\}(\omega)|^2da=C<\infty$;

are satisfied, then the function

$$TF_x:A\times R\to C,\quad TF_x(t,\omega)=\langle x(\tau),K(\tau-t,\omega)\rangle=\int_{-\infty}^{\infty}x(\tau)\cdot K^*(\tau-t,\omega)d\tau$$

is named linear TFR of the finite energy signal $x(\tau)$.[7]

The two variable function $K(u,v)$ is the kernel of the linear TFR. The kernel for the short-time Fourier transform is $K_{\mathrm{STFT}}(\tau,a)=w(\tau)\cdot e^{ja\tau}$. If the window, $w(\tau)$ is Gaussian, then the corresponding TFR is the Gabor transform. The bilinear TFRs of the Cohen's class can be computed for the signal x with the relation

$${}_C\mathrm{TF}_x(t,\omega)=\frac{1}{2\pi}\cdot\int_{-\infty}^{\infty}\int_{-\infty}^{\infty}\int_{-\infty}^{\infty}x\left(s+\frac{\tau}{2}\right)\cdot x^*\left(s-\frac{\tau}{2}\right)\cdot e^{-j(\omega\tau-us+ut)}\cdot f(u,\tau)du\,ds\,d\tau, \tag{1}$$

where $f(u,\tau)$ is another kernel. For the Wigner–Ville TFR this kernel is unitary.[8]

Some of the members of the Cohen's class realize a good localization of the ridges of the analyzed signal. A very good example is the Wigner–Ville distribution.[1]

But for the IF estimation of multi component signals or of signals perturbed by noise, the linear TFRs are more useful due to the absence of the interference terms. The good concentration around the IF law properties of the linear TFRs of signals with double modulation of the form

$$s(t)=A(t)\cdot e^{jb(t)} \tag{2}$$

is known.[2]

2.1 *Spreading the Noise in the Time-Frequency Plane*

To observe this effect a statistical analysis of TFRs is necessary. Such an analysis is already reported.[9] The better TFR is that realizing the higher noise spreading. This spreading effect is maximized if the noise in the TFP is white. When this noise is correlated, its power is concentrated in some regions where the ridges of the TFR of the useful component can be also located. The noise spreading effect is maximized when the TFR used decorrelates the input noise. In the following the linear and bilinear TFRs that decorrelates the input noise are searched. We suppose that the signal to be represented in the TFP, $n(t)$, is a stationary noise.

2.1.1 *The case of linear time-frequency representations*

The linear TFR of a realization of the noise $n(t)$ is

$${}_l\mathrm{TF}_n(t,\omega)=\int_{-\infty}^{\infty}n(\tau)\cdot K^*(\tau-t,\omega)d\tau. \tag{3}$$

The system for the computation of this TFR is a time invariant linear system with the impulse response $K^*(-t,\omega)$, where the frequency, ω, represents a parameter. At any frequency, ω, this system responds to the input signal, $n(t)$, with the signal $n_o(t)$, the linear TFR, ${}_1\mathrm{TF}_n(t,\omega)$, computed at that frequency.

This is a random process with the mean[9]

$$E\{{}_l\mathrm{TF}_n(t,\omega)\}=M_n\cdot\int_{-\infty}^{\infty}K^*(\tau-t,\omega)d\tau, \tag{4}$$

where M_n represents the mean of the noise. The correlation function of the TFR from the relation (3) is

$$E\{{}_l\mathrm{TF}_n(t_1,\omega_1)\,{}_l\mathrm{TF}_n(t_2,\omega_2)\}=\int_{-\infty}^{\infty}\int_{-\infty}^{\infty}K^*(\tau_1-t_1,\omega_1)\cdot K^*(\tau_2-t_2,\omega_2)\cdot R_n(\tau_1-\tau_2)d\tau_1\,d\tau_2, \tag{5}$$

where R represents the correlation operator. For a zero mean white noise with standard deviation, σ, the last relation becomes[9]

$$E\{{}_l\mathrm{TF}_n(t_1,\omega_1)\,{}_l\mathrm{TF}_n(t_2,\omega_2)\}=\sigma^2\cdot\int_{-\infty}^{\infty}K^*(\tau_1-t_1,\omega_1)\cdot K^*(\tau_1-t_2,\omega_2)d\tau_1. \tag{6}$$

So, any linear TFR correlates the input noise. This correlation can be avoided only for discrete linear TFRs. It is well known the whitening effect of the discrete wavelet transform[8] (DWT).

The power of the output signal of the system for the computation of the linear TFR is

$$\begin{aligned}E_{n_o}&=\frac{1}{2\pi}\cdot\int_{-\infty}^{\infty}|N_o(\omega)|^2d\omega\\&=\frac{1}{2\pi}\cdot\int_{-\infty}^{\infty}|N(\omega)|^2|\Im\{K^*(-t,\omega)\}(\omega)|^2d\omega\\&\leqslant\frac{1}{2\pi}\cdot\int_{-\infty}^{\infty}|N(\omega)|^2d\omega\cdot\int_{-\infty}^{\infty}|\Im\{K^*(-t,\omega)\}(\omega)|^2d\omega^{3)}\\&=\frac{1}{2\pi}\cdot\int_{-\infty}^{\infty}|N(\omega)|^2d\omega=E_n.\end{aligned} \tag{7}$$

So, at any frequency, the power of the signal $n_o(t)$ is inferior to the power of the signal $n(t)$. Hence, the linear TFR realizes a spreading of the noise in the TFP. Unfortunately, with the exception of the DWT, the linear TFRs do not have the decorrelation property. It is recognized[5] that the Gabor TFR realizes the better localization in the TFP (see the Heisenberg principle). This is the reason why this linear TFR was selected for the computation of the new TFR proposed in this paper.

2.1.2 *The case of bilinear time-frequency representations*

A Cohen's class TFR of the signal $n(t)$ can be computed using the relation (1). Its mean is[9]

$$E\{{}_C\mathrm{TF}_n(t,\omega)\}=\frac{1}{2\pi}\cdot\int_{-\infty}^{\infty}\int_{-\infty}^{\infty}\int_{-\infty}^{\infty}R_n(\tau)\cdot e^{-j(\omega\tau-us+ut)}\cdot f(u,\tau)\,du\,ds\,d\tau. \quad (8)$$

If $n(t)$ is a zero mean white noise with standard deviation σ then the mean of its bilinear TFR becomes[9]

$$E\{{}_C\mathrm{TF}_n(t,\omega)\}=\sigma^2\cdot f(0,0). \quad (9)$$

If $n(t)$ is a zero mean white noise with standard deviation σ, the correlation of its Cohen's class TFR is[9]

$$E\{{}_C\mathrm{TF}_n(t_1,\omega_1)\,{}_C\mathrm{TF}_n(t_2,\omega_2)\}=-\frac{\sigma^4}{2\pi}\cdot\mathfrak{I}_2\{f(u_2,\tau_1)\cdot f(-u_2,\tau_1)\}(\omega_1+\omega_2,t_1+t_2)+\sigma^4\cdot f(0,0)+\frac{\sigma^4}{\pi}\cdot\mathfrak{I}_2\{f(u_2,\tau_2)f(-u_2,\tau_2)\}\times(\omega_2-\omega_1,t_2-t_1), \quad (10)$$

where $\mathfrak{I}_2$ represents the two-dimensional Fourier transform. For the case of the Wigner–Ville TFR, the last relation becomes

$$E\{\mathrm{TF}_n^{W-V}(t_1,\omega_1)\mathrm{TF}_n^{W-V}(t_2,\omega_2)\}=4\pi\sigma^4\cdot\delta(\omega_2-\omega_1)\cdot\delta(t_2-t_1)+\sigma^4-2\pi\sigma^4\cdot\delta(\omega_2+\omega_1)\cdot\delta(t_2+t_1). \quad (11)$$

Hence, the Wigner–Ville TFR of a zero mean white noise, with standard deviation σ, is a two-dimensional random process, very close to a two dimensional white noise. So, generally, the Cohen's class TFRs correlates the input signal but the Wigner–Ville TFR is an exception. Because the Wigner–Ville distribution is a spectro-temporal density of energy that do not correlates the input noise, it posses the noise power spreading in the TFP effect, that represents the subject of this paragraph. This is the reason why this member of the class of bilinear TFRs was selected for the construction of the new TFR proposed in this paper.

2.2 *A New Time-Frequency Representation*

To combine the advantages of the Gabor TFR (the good localization and the absence of interference terms), with the advantages of the Wigner–Ville TFR (the good concentration in the TFP and the noise spreading effect), the following algorithm can be used:

1. The computation of the Gabor transform of the signal $x(t)$, $\mathrm{TF}_x^G(t,\omega)$. The noise power is diffused in the TFP. Only a small part of this power affects the ridges of $\mathrm{TF}_s^G(t,\omega)$.
2. The filtering of the image obtained, $y(t,\omega)=\mathrm{TF}_x^G(t,\omega)$, with the aid of a filter inspired from the hard-thresholding filter. This system has the following input–output relation:
$$z(t,\omega)=\begin{cases}1, & \text{if } |y(t,\omega)|\geqslant \mathrm{tr},\\ 0, & \text{if } |y(t,\omega)|<\mathrm{tr},\end{cases} \quad (12)$$
where tr is a threshold. This threshold value is selected using a procedure described in Sec. 4.1. Doing so, a prototype TFR, $z(t,\omega)$, the denoised version of the TFR $y(t,\omega)$, is obtained. The denoising operation decreases the amount of noise that perturbs the ridges of $\mathrm{TF}_s^G(t,\omega)$ and brings to zero the values in the rest of the TFP. This is the reason why the interference terms of the bilinear TFR that will be used in the following step will be reduced in the final step of this method.
3. The computation of the Wigner–Ville TFR of the signal $x(t)$, $\mathrm{TF}_x^{W-V}(t,\omega)$. The goal of this step is to enhance the localization on the curve of IF of the signal $s(t)$, in the TFP.
4. The new TFR, $\mathrm{TF}_x^{\mathrm{new}}(t,\omega)$ that represents the subject of this paragraph, is computed by the multiplication of the modulus of the prototype TFR, $z(t,\omega)$ with $\mathrm{TF}_x^{W-V}(t,\omega)$. The effect of this multiplication is the reduction of the interference terms of the Wigner–Ville distribution and the very good localization of the ridges of the result in the TFP. All the interference terms positioned far enough with respect to the corresponding auto terms and in different positions like other auto terms will be cancelled. The interference terms having the same position like other auto terms are not cancelled, but their presence do not affects the instantaneous frequency estimation, due to the ridges estimation mechanism described in the following paragraph.

Simulations proving the efficiency of this method for the interference terms reduction are already reported,[10] but the use of this new TFR for the IF estimation is proposed for the first time in this paper. Another new TFR, very useful for the instantaneous frequency estimation is the S-method.[11,12] By different parametrizations, this TFR can become the Gabor TFR or the Wigner–Ville TFR. The S-method can be efficiently used for the suppression of the interference terms, even when these terms are superposed on auto terms. It was used for the instantaneous frequency estimation of signals perturbed by noise.[11,12] For the detection of the ridges of the S-method very simple detectors were used.[11,12] The construction of those detectors is based on Boolean operators, a type of mathematical morphology operators.

3 The Role of the Mathematical Morphology

Some mathematical morphology operators can be used to estimate the ridges of the new TFR, proposed in this paper. There are two goals of this estimation procedure: to continue the denoising of the new TFR and to extract the projection of the ridges of this TFR on the TFP.

The first mathematical morphology operator used in the ridges detection method, proposed in this paper is the conversion in binary form.[13] This operator realizes a threshold-

ing of the TFR. In fact this is a new denoising procedure. The second mathematical morphology operator used in the proposed detection method is the dilatation operator.[13] Its role is to compensate the connectivity loose, produced by the conversion in binary form. Finally, the last mathematical morphology operator used is the skeleton.[13] It produces the ridges estimation.

4 The New Algorithm

The algorithm that represents the aim of this paper has the following steps:

1. The new time-frequency representation of the signal $x(t)$, $\mathrm{TF}_x^{\mathrm{new}}(t,\omega)$, is computed.
2. Its image is converted in binary form.
3. To compensate the connectivity loose, a dilatation of the image obtained is performed obtaining a new image.
4. Applying the skeleton operator to the last image an estimation of the instantaneous frequency of the signal s(t) is obtained. This image represents the result of the proposed estimation method.

For the case of three components, when the second one is exactly in the middle between the first and the third one, an interference term (produced by the first and the third component) will be superposed to an auto term (the second component). The new TFR will represent all the three auto terms, the second being affected by the interference term. Their skeletons will give the estimations of their instantaneous frequencies. In fact only the connectivity of the TFR of the second auto term is affected by the interference term. Using a dilatation, this connectivity loose is compensated. So, the presence of the interference term will not affect the estimation quality.

Performances expected: An IF estimation method is better than other if for the same input signal it has a higher precision. This precision is dependent on some parameters belonging to three distinct categories: parameters depending on the input signal, parameters specific to the TFR used, parameters of the projection mechanism.

The parameters depending on the input signal are: the nature of its useful component, the nature of its noise component, its SNR.

The parameters of the TFR used are: the energy concentration around the IF curve, its resolution-the capacity to separate two different components of the input signal, its capacity to spread the noise.

The parameters of the projection mechanism are of statistical nature.

A performance measure, p, for the IF estimation methods, based on the use of TFRs, is already reported.[14] At every frequency, ω, this performance measure depends on the following parameters of the TFR of each component: the side lobe magnitude, $A_S(t)$, the main lobe magnitude, $A_M(t)$, the cross-term magnitude, $A_X(t)$, the instantaneous bandwidth, $v_i(t)$, the IF, $f_i(t)$ and the frequency resolution, $D(t)$, a separation measure, between the components' main lobes[14]

$$D(t)=1-\frac{v_i(t)}{\Delta f_i(t)},$$

where $\Delta f_i(t)$ represents the difference between the IF of the two main lobes. The expression of this performance measure is

$$p(t)=1-\frac{1}{3}\left[\frac{A_S(t)}{A_M(t)}+\frac{1}{2}\frac{A_X(t)}{A_M(t)}+1-D(t)\right]. \tag{13}$$

This performance measure can be used to select the better quadratic TFR for the IF estimation of a given signal.[14] A good candidate can be the Modified B distribution.[14] But this measure depends on the input signal, because $A_X(t)$ and $D(t)$ are very signal dependents. So, another idea was tested, the construction of an adaptive quadratic TFR. The kernel of the quadratic TFR can be modified along the estimation procedure to maximize $p(t)$. A new adaptive TFR was recently proposed.[3] Another is the S-method.[11,12] Unfortunately, like any adaptive procedure, the computation of those TFRs requires a large number of operations. The performance measure in (13) can be computed also for the new TFR proposed in this paper. The hard thresholding filter used for the computation of the new TFR has a windowing effect. It produces the partition of the TFP into two categories of frequencies: the frequencies where the new representation is equal with zero at every moment and the frequencies, ω, where there are time intervals corresponding to values not null of the new TFR. Let $B(\omega,t)$ be the characteristic function of those intervals, for any ω. This function's expression strongly depends on the selection of the threshold, tr, in relation (12). It also depends on the length of the window used for the computation of the Gabor TFR.

Let

$${}_{\omega}B(t)=\bigcup_{u}B(u,t).$$

The expression of the new TFR side lobe is

$$A_S(t)={}^{W-V}A_S(t)\,{}^{G}A_M(t)\,{}_{\omega}B(t), \tag{14}$$

where ${}^{W-V}A_S(t)$ represents the side lobe magnitude of the Wigner–Ville TFR and ${}^{G}A_M(t)$ represents the main lobe of the Gabor TFR. The expression of the main lobe of the new TFR, proposed in this paper, is

$$A_M(t)={}^{W-V}A_M(t)\,{}^{G}A_{\mathrm{M}}(t), \tag{15}$$

where ${}^{W-V}A_M(t)$ is the main lobe of the Wigner–Ville TFR. So the first term in the right-hand side parentheses in (13) becomes

$$T_1(t)=\frac{A_S(t)}{A_M(t)}=\frac{{}^{W-V}A_S(t)\,{}_{\omega}B(t)}{{}^{W-V}A_M(t)}={}^{W-V}T_1(t)\,{}_{\omega}B(t). \tag{16}$$

The contribution of the interference terms of the new TFR has the expression

$$A_X(t)={}^{W-V}A_X(t)\,{}^{G}A_{\mathrm{M}}(t)\,{}_{\omega}B(t), \tag{17}$$

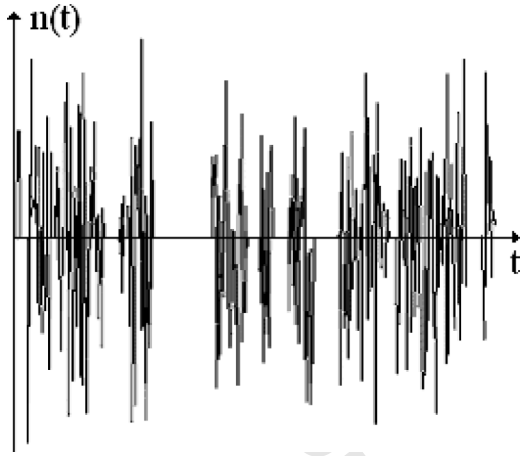

Fig. 1 The waveform of the noise used in the first two simulation examples.

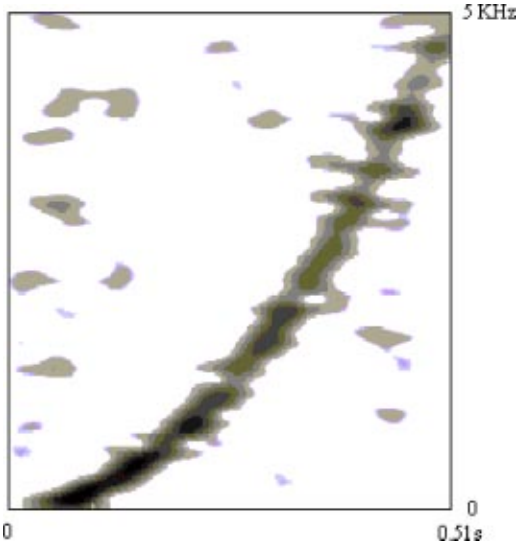

Fig. 2 The modulus of the Gabor transform of the signal used in the first simulation example, $|\mathrm{TF}_{x_1}^{G}(t,\omega)|$.

where ${}^{W-V}A_X(t)$ represents the cross-term magnitude of the Wigner–Ville TFR. Hence the second term of the parenthesis of the performance measure in (13) becomes for the new TFR proposed in this paper:

$$T_2(t)=\frac{1}{2}\frac{{}^{W-V}A_X(t)}{{}^{W-V}A_M(t)}\,{}_{\omega}B(t)={}^{W-V}T_2(t)\,{}_{\omega}B(t). \tag{18}$$

The components' separation measure of the new TFR can also be expressed in the form

$$D(t)={}^{W-V}D(t)\,{}_{\omega}B(t). \tag{19}$$

So the performance measure of the new TFR can be written in the form

$$p^{\mathrm{new}}(t)=\begin{cases}{}^{W-V}p(t), & \text{if } {}_{\omega}B(t)=1\\ 1, & \text{if } {}_{\omega}B(t)=0\end{cases}. \tag{20}$$

The last relation proves the superiority of the new TFR versus the Wigner–Ville TFR. The reduced surface occupied by the support of the function ${}_{\omega}B(t)$ in the TFP, even when the noise component of the acquired signal is present, ensures a high precision to the IF estimation method, proposed in this paper. Of course the expression of ${}_{\omega}B(t)$ is signal dependent but this dependency is wicker than the signal dependency of the Wigner–Ville TFR.

The performance measure already analyzed do not takes into account the effect of the noise. Recently an analysis of this effect was done.[4] The estimation error produced by the approximation of the law of the IF with the ridges of a quadratic TFR is computed.[4] Exact expressions for the IF estimator bias and variance in the case of white stationary and white not stationary noises are also derived. The influence of the SNR of the analyzed signal on the variance of the estimation error is also studied. This variance decreases when the SNR increases. Hence, an important parameter of the estimation method is the inferior bound of the SNR that produces an acceptable estimation variance. An example for such a bound value is of -0.7 dB.[4] Unfortunately any ridges' projection on TFP mechanism is not considered in this reference. Because the basic morphological operators are robust against noise, the projection mechanism proposed here decreases the estimation variance. Indeed the erosion and the dilation are morphological operators robust against noise.[15,16] Because the skeleton can be computed making repeated erosions, this is also a morphological operator robust against noise. So, using the estimation method proposed here, better results than those already reported,[3,4] can be expected. The performances of the proposed IF estimation method strongly depends on the expression of the function ${}_{\omega}B(t)$. The parameters of this function are the length of the window used for the computation of the Gabor TFR and the value of the threshold tr, defined in (12). These parameters must be selected to minimize the surface of the support of ${}_{\omega}B(t)$. Generally, the window's length is selected on the basis of information about the signals $s(t)$ and $n(t)$. In this paper is considered the case when any information about these signals is accessible. This is the reason why a moderate window's length is recommended. This length is obtained dividing the length of the signal $x(t)$ to 4. The value recommended for the interwindow spacing is of 1. Hence, the only parameter relevant for the minimization of the surface of the support of ${}_{\omega}B(t)$, is the threshold's value tr. The selection of this parameter can be done using estimations of the parameters of the signals $\mathrm{n}(t)$ and $s(t)$. David Donoho introduced the hard thresholding filter, in connection with a denoising application.[21] Because in this application all the noise must be removed, the threshold's value is selected proportional with the variance of the noise $n(t)$. This is not an appropriate selection for the processing of signals with low SNR.

The ridges detectors used in cooperation with the S-method,[11,12] use also a kind of hard thresholding filter. The threshold's value selection procedure recommended in these references is based on parameters of the signal $x(t)$, the maximum absolute value of $\mathrm{TF}_x^G(t,\omega)$ divided by 5, or the square root of the power of the S-method of $x(t)$, divided by 25.[11,12] The surface of the support of ${}_{\omega}B(t)$ is

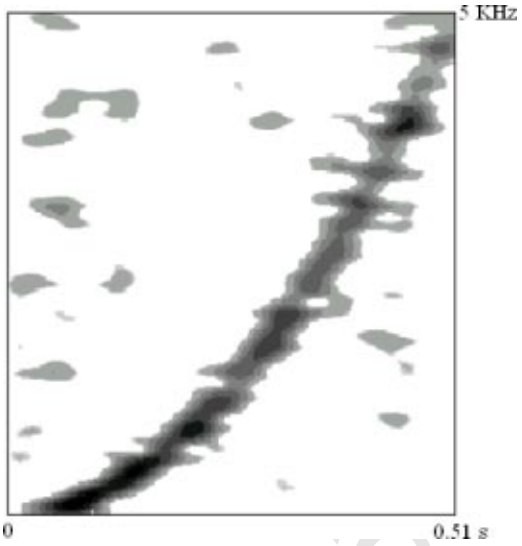

Fig. 3 The denoised Gabor transform of the signal used in the first simulation example, $z_1(t,\omega)$.

inverse proportional with the value tr. But there is a superior bound tr_0. If tr is greater than that bound, then the connectivity of $\mathrm{TF}_x^G(t,\omega)$ is broken. The value of this bound depends on the variations of the amplitude of $x(t)$. Is difficult to estimate this bound without additional information about $s(t)$ and $n(t)$. For the experiments reported in the next section the following threshold's value was used:

$$\mathrm{tr}=\frac{\max_{(t,\omega)}\{|\mathrm{TF}_x^G(t,\omega)|\}}{5}.$$

This selection is not critical, taking into account the capacity of connectivity reconstruction of the method proposed.

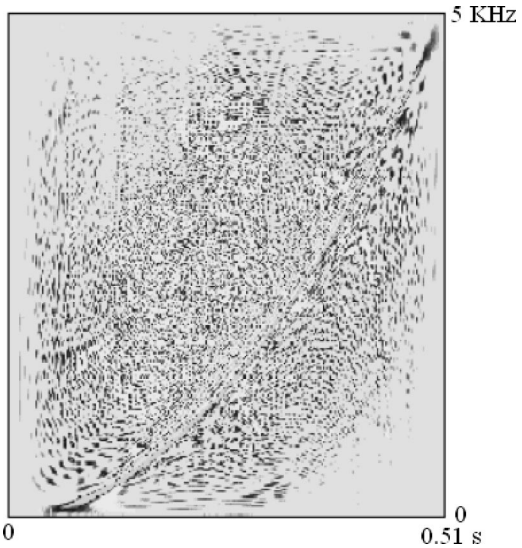

Fig. 4 The modulus of the Wigner–Ville transform of the signal used in the first simulation example, $|\mathrm{TF}_{x_1}^{W-V}(t,\omega)|$.

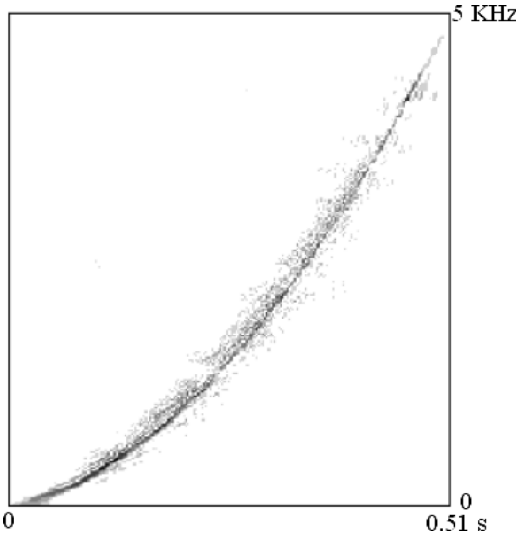

Fig. 5 The modulus of the new TFR of the signal used in the first simulation example, $|\mathrm{TF}_{x_1}^{\mathrm{new}}(t,\omega)|$.

5 Simulation Results

In the following are presented some simulation results.

5.1 *First Example*

The signal $s_1(t)$ is a monocomponent signal with quadratic modulation law and constant amplitude

$$s_1(t)=\sin\left(\frac{512\cdot\pi}{3}\cdot t^3\right) \quad t\in[0,0.512].$$

The perturbation $n(t)$ is a train of noise pulses. This kind of perturbation appears frequently in practice. A realization of this random process is represented in Fig. 1.

The acquired signal has a low SNR, of value 1.34. In Fig. 2 is represented the modulus of the Gabor transform of the signal $x(t)$. Because $n(t)$ is a correlated noise and be-

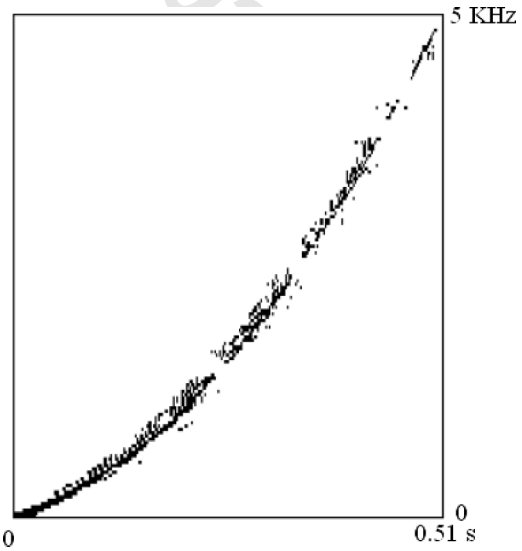

Fig. 6 The image obtained after the conversion in binary form of the image in Fig. 5.

PROOF COPY 511502JEI

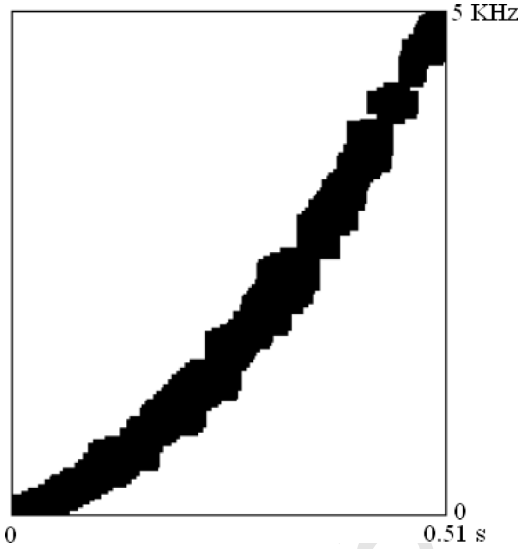

Fig. 7 The image obtained after the dilatation of the image in Fig. 6.

cause the Gabor TFR does not have the decorrelation property, some energy concentrations apart from $TF_{s_1}^{G}(t,\omega)$ can be observed. After the filtering with the filter described in relation (12) is obtained a new result, with the modulus presented in Fig. 3. The denoising effect can be observed. In Fig. 4 can be viewed the image of the absolute value of the Wigner–Ville TFR of the considered signal. It is very difficult to observe $TF_{s_1}^{W-V}(t,\omega)$ in this figure. The modulus of the new TFR is presented in Fig. 5. The quality enhancement versus Figs. 1 and 3 is obvious. Converting this image in binary form (see Fig. 6), after a dilatation, (see Fig. 7) and the application of the skeleton operator, the result of the estimation method, presented in Fig. 8, is obtained. The connectivity loose can be observed comparing Figs. 5 and 6. After the application of the dilatation operator the connectivity is reconstructed. This effect can be observed comparing Figs. 6 and 7.

Comparing the IF curve of the signal $s(t)$ with the result obtained in Fig. 8, the estimation error can be appreciated. For this example the maximum error appears at the frequency 3748 Hz and at the moment 0.464 s, having an absolute value of 142 Hz. So the maximum relative error is of 0.0284.

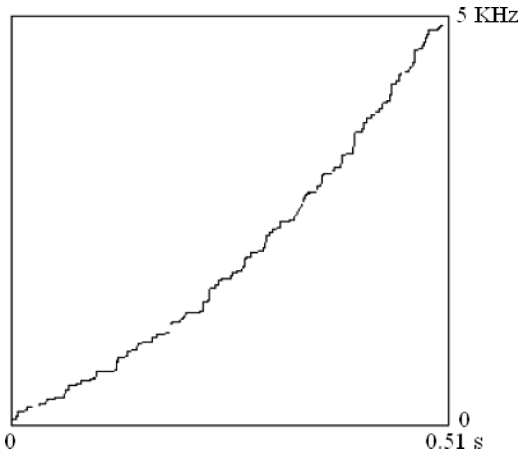

Fig. 8 The skeleton of the previous image.

Fig. 9 The Wigner–Ville TFR of the acquired signal for the second simulation example, $TF_{x_2}^{W-V}(t,\omega)$.

5.2 *Second Example*

The signal $s_2(t)$ is composed of two chirps with linear modulation laws and constant amplitudes,

$$s_2(t)=\sin\left(\frac{512\cdot\pi}{2}\cdot t^2\right)+\sin\left(\frac{512\cdot\pi}{3}\cdot t^2\right)\qquad t\in[0,0.512].$$

The perturbation is the same as in the first example. The SNR of the acquired signal is of 2.9. In Fig. 9 is presented the Wigner–Ville TFR of the acquired signal. The result of the proposed estimation method can be seen in Fig. 10.

Comparing the IF curve of the signal $s(t)$ with the result obtained in Fig. 10, the estimation error can be appreciated. For this example the maximum relative error is of 0.0428.

Some results obtained using the signals already analyzed, with different SNR, are presented in Table 1. In the second column the SNR values used in every case are indicated. The third and the forth columns contains the points of the TFP where the maximal estimation errors were appeared. Their absolute values are presented in the fifth column. The last column contains the corresponding relative errors. The good precision of the proposed estimation method can be observed analyzing the table. Despite the small values of the SNR, 0.86 for the first experiment and 1.86 for the second, the maximum relative errors are small, 0.028 for the first experiment and 0.043 for the second one. When the SNR is small, the estimation is less precise for the case of multicomponent signals. When the SNR is high the difference between the IF estimation of two signals Quad Chirp (monocomponent) and Two Chirp (multicomponent) becomes invisible. Analyzing the last figure it can be observed that the proposed method has difficulties at the

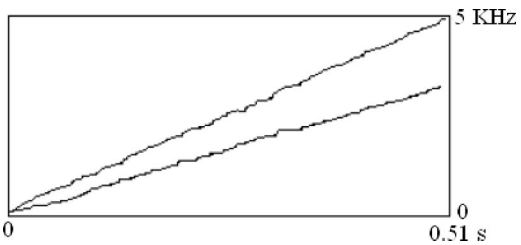

Fig. 10 The result of the IF estimation for the second simulation example.

Table 1 The SNR dependency of the IF estimation precision for the signals in the examples already presented.

Signal	SNR	Frequency (kHz)	Time (s)	Absolute error (Hz)	Relative error
Quad chirp first experiment	0.8608	3.74	0.0446	142	0.0284
	5.3789	3.85	0.0452	142	0.0284
	134.4942	3.89	0.0455	107	0.0214
Two chirp second experiment	1.8609	0.59	0.0125	214	0.0428
	11.6308	0.81	0.0132	107	0.0214
	290.769	0.81	0.0135	71	0.0142

intersections of the TFRs of different components of the signal $x(t)$. At the intersections, the computation of the good skeleton is more difficult. This is a problem under the current investigation of the authors.

5.3 *Third Example*

In the following a comparison with another IF estimation method[12] is done. A synthetic car engine signal, proposed in this reference, is considered. In fact this signal is very closed to a real combustion engine signal. Its expression is

$$s_3(t)=2\cdot\sum_{k=1}^{5}A_k(t)\cos(\varphi_k(t))+n(t)\qquad t\in[0,1],$$

where

$$\varphi_k(t)=c_2(k)\cdot t^2+c_1(k)\cdot t+\Phi(k)$$

and

$$A_k(t)=A(k)\cdot e^{-d(k)\cdot t},$$

where $A=[12\,8\,6\,4\,4.5]$, $d=[8\,6\,6\,5\,5.8]$, $\Phi(k)$ are uniformly distributed within $[0,2\pi]$ and $n(t)$ is a zero mean white noise with $\sigma=0.1$. In this case the input SNR value is 5019.8. The phases of this experiment are presented in Figs. 11–16.

The image of the Gabor RTF of the considered signal can be viewed in Fig. 11. The five parallel chirps composing the signal can be observed. Filtering this image with the aid of the filter in relation (12), the image in Fig. 12 is obtained. The image of the Wigner–Ville RTF of the considered signal is presented in Fig. 13. The superposition of auto terms and interference terms can be observed comparing Figs. 11 and 13. In Fig. 14 is presented the image of the new TFR of the signal $s_3(t)$, proposed in this paper, converted in binary form. It can be observed, comparing the last two figures, that a great number of interference terms were eliminated. The effect of the superposition of some interference terms on auto terms is the connectivity loose. This is the reason why a dilatation operator was applied to the image in Fig. 14 obtaining the image from Fig. 15. Applying the skeleton, the IF estimation of the signal $s_3(t)$, presented in Fig. 16 is obtained. The quality of the estimation is similar with the IF estimation quality of the same signal, based on the use of the S-method.[11] Repeating the same experiment for a smaller SNR, 4.53, the result presented in Fig. 17 is obtained.

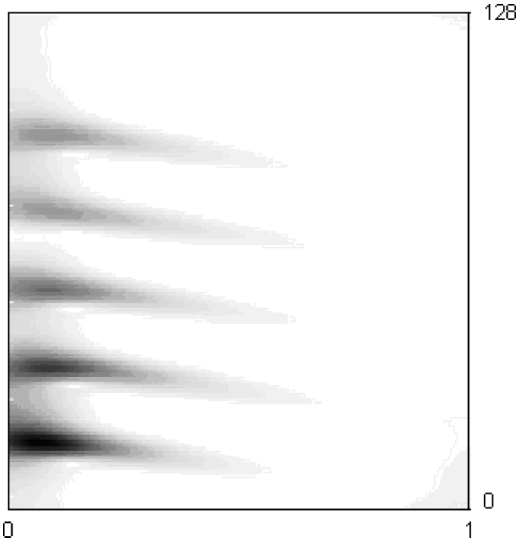

Fig. 11 The modulus of the Gabor transform of the signal used in the third simulation example, $|\mathrm{TF}^{G}_{x_3}(t,\omega)|$.

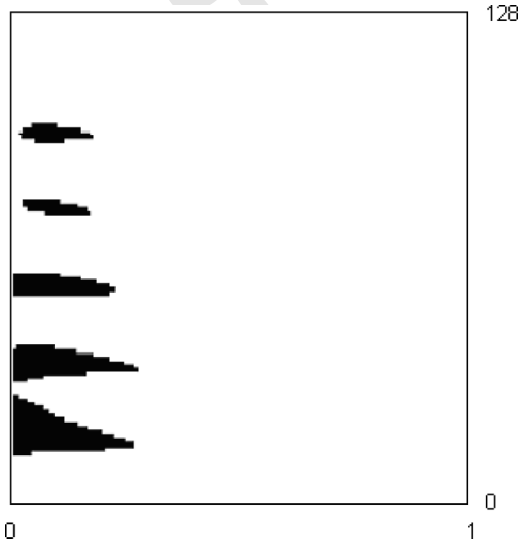

Fig. 12 The denoised Gabor transform of the signal used in the third simulation example, $z_3(t,\omega)$.

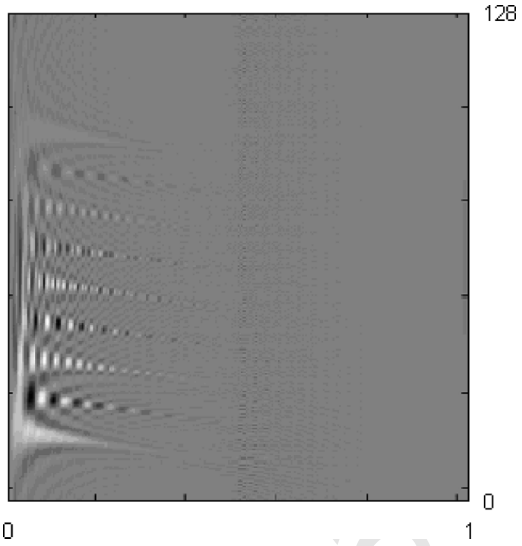

Fig. 13 The modulus of the Wigner–Ville transform of the signal used in the third simulation example, $|\mathrm{TF}_{x_3}^{W-V}(t,\omega)|$.

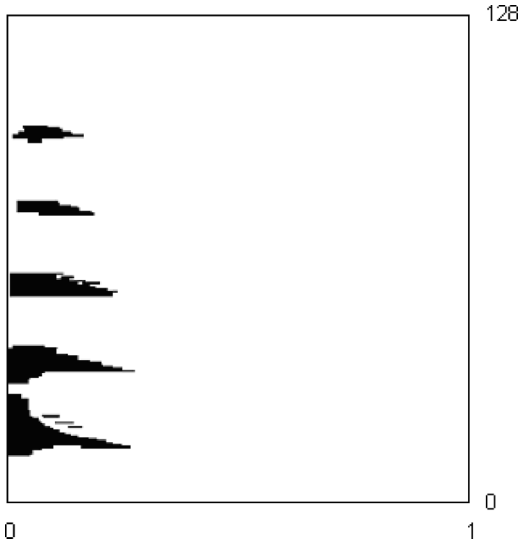

Fig. 15 The image obtained after the dilatation of the image in Fig. 14.

The images in Figs. 16 and 17 quite resemble. So, the proposed, IF estimation method is resilient to noise and can be used for the analysis of combustion engines.

6 Conclusions

The IF estimation method proposed in this paper has performances similar or better than other methods.[2–4,6,17–20] The method is quite universal, the SNR of the input signal can be very small and the result is not affected by the statistics of the perturbation $n(t)$. For example similar results for the first two simulation examples can be obtained for white Gaussian noise.

For signals, $s(t)$, with constant amplitude, using the method proposed in this paper, the reconstruction could be also achieved. So, this method can be regarded like a denoising method for frequency-modulated signals with constant amplitude. Knowing the IF law, the frequency-modulated signal with constant amplitude can be synthesized very easy. For the case of the use of the continuous wavelet transform a similar conclusion is reported.[6] Such a method outperforms the majority of denoising methods for the frequency-modulated signals being able to reconstruct very low SNR signals. Other SNR enhancement methods, like for example the Donoho denoising method,[21] are not designed for the treatment of low SNR signals.

The multiplication of a linear and a bilinear TFR conducts to an important reduction of the interference terms (compare for example Figs. 3 and 4). The class of morphological operators used in the proposed estimation method can be extended.

The IF estimation method proposed in this paper is based on the conjoint use of two very modern theories, that of TFRs and that of mathematical morphology. This con-

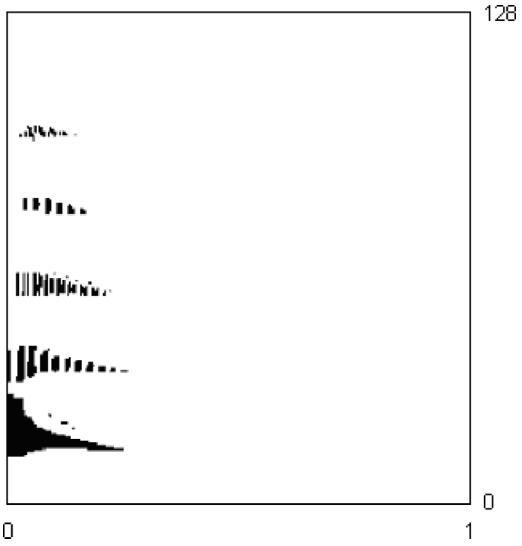

Fig. 14 The image of the modulus of the new TFR of the signal used in the third simulation example, $|\mathrm{TF}_{x_3}^{\mathrm{new}}(t,\omega)|$, after conversion in binary form.

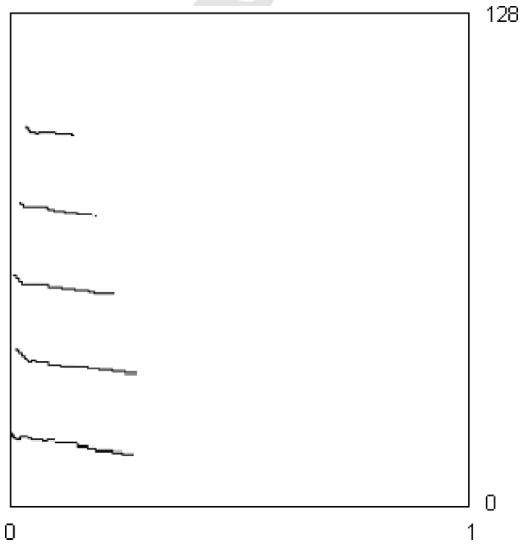

Fig. 16 The skeleton of the image in Fig. 15.

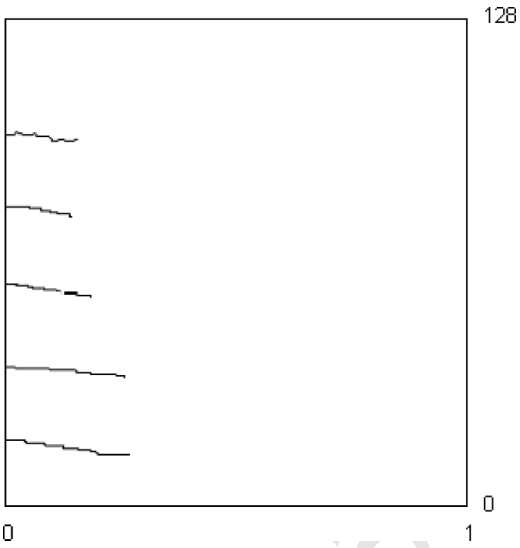

Fig. 17 The result of the third simulation example for a smaller SNR.

nection is very important because the TFRs are generally used for the processing of signals with only one dimension and the mathematical morphology is used to process images. Our proposition permits to use the image processing techniques to the analysis of mono dimensional signals. This strategy permits the enhancement of the set of signal processing methods with the aid of some methods developed in the context of image processing. The estimation method proposed in this paper can be used in a lot of applications. Some of them, like radar, sonar, or telecommunications are already recognized as applications of the TFR theory.

Acknowledgments

The authors are thankful to the reviewers for very thorough comments that help to improve the manuscript. This work is a result of a grant of the Romanian National Scientific Research Council.

References

1. B. Boashash, P. O. Shea, and M. J. Arnold, ''Algorithms for Instantaneous Frequency Estimation: A Comparative Study,'' *Proc. SPIE* ■, ■–■ (1990).
2. N. Delprat, B. Escudie, P. Guillemain, R. Kronland-Martinet, Ph. Tchamitchian, and B. Torresani, ''Asymptotic wavelet and Gabor analysis: Extraction of instantaneous frequencies,'' *IEEE Trans. Inf. Theory* **38**, 644–664 (1992).
3. Z. M. Hussain and B. Boashash, ''An adaptive instantaneous frequency estimation of multicomponent FM signals using quadratic time-frequency distributions,'' *IEEE Trans. Signal Process.* **50**, 1866–1876 (2002).
4. V. N. Ivanovic, M. Dakovic, and L. Stankovic, ''Performance of Quadratic Time-Frequency Distributions as Instantaneous Frequency Estimators,'' *IEEE Trans. Signal Process.* **51**, 77–89 (2003).
5. P. Flandrin, *Representation Temps-Fréquence*, Hermes (1993).
6. R. A. Carmona, W. L. Hwang, and B. Torresani, ''Multiridge detection and time-frequency reconstruction'' (preprint, June 21, 1995).
7. P. Gavruta and A. Isar, ''Time-frequency representations: A unitary presentation,'' in *Proc. of the International Symposium, Etc '94*, Vol. 3, pp. 25–30, Timisoara, Romania (September 1996).
8. M. Borda and D. Isar, ''Whitening with Wavelets,'' in *Proc. of ''EC-CTD. 97'' Conference*, Budapest (August 1997).
9. A. Isar, D. Isar, and M. Bianu, ''Statistical analysis of two classes of time-frequency representations,'' *Facta Universitatis, series Electronics and Energetic* **16**, 115–134 (2003).
10. M. Bianu and A. Isar, ''The reduction of interference terms in the time-frequency plane,'' in Proc. of the International Symposium SCS'2003, pp. 461–464, Iasi, Romania (July 10–11, 2003).
11. S. Stankovic and L. Stankovic, ''An architecture for the realization of a system for time-frequency signal analysis,'' *IEEE Trans. Circuits Syst., II: Analog Digital Signal Process.* ■ , 600–604 (1997).
12. L. Stankovic and J. F. Boehme, ''Time-frequency analysis of multiple resonances in combustion engine signals,'' *Signal Process.* **79**, 15–28 (1999).
13. F. Preteux, ''Description et intérprétation des images par la morphologie mathématique. Application a l'image médicale,'' These de doctorat d'Etat, Université Paris VI (1987).
14. B. Boashash, ''Resolution measure criteria for the objective assessment of the performance of quadratic time-frequency distributions,'' *IEEE Trans. Signal Process.* **51**, 1253–1263 (2003).
15. D. Schonfeld and J. Goustias, ''Optimal Morphological Pattern Restoration of Noisy Binary Images,'' *IEEE Trans. Pattern Anal. Mach. Intell.* **13**, 14–29 (1991).
16. D. Schonfeld, ''Optimal structuring elements for the morphological pattern restoration of binary images,'' *IEEE Trans. Pattern Anal. Mach. Intell.* **16**, 589–601 (1994).
17. R. Carmona, B. Torresani, and W. L. Hwang, ''Identification of chirps with continuous wavelet transform,'' in *Wavelets and Statistics*, A. Antoniades and G. Oppenheim, Eds., pp. 95–108, Springer Verlag, New York (1995).
18. C. Gordan, M. Regep, and I. Nafornita, ''Estimating and interpreting the instantaneous frequency of a frequency modulated signal. Part 1. Fundamentals and algorithms,'' Scientifically Bulletin of ''Politehnica'' University, Timisoara, Tome 43, pp. 175–184 (1998).
19. C. Gordan, M. Regep, and I. Nafornita, ''Estimating and interpreting the instantaneous frequency of a frequency modulated signal. Part 2. Practical results,'' Scientifically Bulletin of ''Politehnica'' University, Timisoara, Tome 43, pp. 185–190 (1998).
20. T. Asztalos, A. Marina, and A. Isar, ''A new algorithm for the estimation of the instantaneous frequency of a signal perturbed by noise,'' in *Proc. of International Conference MTNS 2000*, Perpignan, France (17–25 June, 2000).
21. D. L. Donoho, ''De-noising by soft thresholding,'' Technical Report No. 409, Stanford University (December 1992).

Monica Borda earned her PhD in 1987, in the Politechnical Institute of Bucharest, Romania. Currently she is a Professor in Information Theory and Coding, and Telecommunications in Technical University of Cluj-Napoca, Romania. She is also working as a PhD advisor in Engineering and Telecommunications. Professor Borda's research areas include information theory and coding, signal processing, watermarking and cryptography.

Ioan Nafornita (M'68) received his BS, MEE, and PhD in electronics in 1965, 1968, and 1981, respectively, from ''Politehnica'' University, Timisoara, Romania. He is currently a Professor, leading the Communications Department of the Electronics and Telecommunications Faculty at the ''Politehnica'' University, Timisoara, Romania. He is also working as a PhD advisor in Engineering and Telecommunications. His current research interests are in the area of statistical signal processing and time-frequency representations.

Dorina Isar (M'80) received her BS, MEE, and PhD in electronics in 1977, 1980, and 1998, respectively, from ''Politehnica'' University, Timisoara, Romania. She is currently an Associated Professor in the Applied Electronics Department of the Electronics and Telecommunications Faculty at the ''Politehnica'' University, Timisoara, Romania. Her current research interests are in the area of digital signal processing and wavelet signal processing.

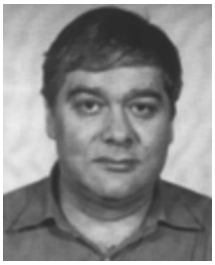

Alexandru Isar (M'82) received his BS, MEE, and PhD in electronics in 1979, 1982, and 1993, respectively, from "Politehnica" University, Timisoara, Romania. He is currently a Professor in the Communications Department of the Electronics and Telecommunications Faculty at the "Politehnica" University, Timisoara, Romania. His current research interests are in the area of digital signal processing and time-frequency representations.